

Recent results of measurements of evaporation residue excitation functions for $^{19}\text{F}+^{194,196,198}\text{Pt}$ and $^{16,18}\text{O}+^{198}\text{Pt}$ systems with HYRA spectrometer at IUAC

B.R. Behera^{1,a}

¹*Department of Physics, Panjab University, Chandigarh 160014, India*

Abstract. In this talk results of the evaporation residue (ER) cross sections for the $^{19}\text{F}+^{194,196,198}\text{Pt}$ (forming compound nuclei $^{213,215,217}\text{Fr}$) and $^{16,18}\text{O}+^{198}\text{Pt}$ (forming compound nuclei $^{214,216}\text{Rn}$) systems measured at Hybrid Recoil mass Analyzer (HYRA) spectrometer installed at the Pelletron+LINAC accelerator facility of the Inter University Accelerator Center (IUAC), New Delhi are reported. The survival probabilities of ^{215}Fr and ^{217}Fr with neutron numbers $N = 126$ are found to be lower than the survival probabilities of ^{215}Fr and ^{217}Fr with neutron numbers $N = 128$ and 130 respectively. Statistical model analysis of the ER cross sections show that an excitation energy dependent scaling factor of the finite-range rotating liquid drop model fission barrier is necessary to fit the experimental data. For the case of $^{214,216}\text{Rn}$, the experimental ER cross sections are compared with the predictions from the statistical model calculations of compound nuclear decay where Kramer's fission width is used. The strength of nuclear dissipation is treated as a free parameter in the calculations to fit the experimental data.

1 Introduction

Evaporation residue (ER) in heavy-ion induced fusion reactions are formed as the outcome of the competition between fission and various particles and γ evaporation channel of the compound nucleus (CN). ER cross sections serve as a sensitive probe to investigate the fission dynamics particularly in the pre-saddle region [1,2]. ER cross sections for heavy systems are also an important indicator to the possibility of formation of super heavy elements in fusion reactions [3]. Stability of heavy nuclei against fission is also a topic of considerable interest in contemporary nuclear physics research. The main reason for this interest is the possibility of synthesizing super heavy elements (SHE) which are predicted to be stable due to shell effects. It is predicted that the next neutron shell closure after $N=126$ will be at $N=184$ and it is expected that this neutron shell closure will be a contributing factor for the stability of a SHE in the mass region $A \sim 300$. It thus becomes important to know to what extent shell closure contributes to the stability of a heavy nucleus against fission. Though shell closure effects give rise to fission barriers typically of the order of a few MeV, the above question arises because other nuclear properties such as the level density and the ground state deformation can also influence the fission process in addition to the fission barrier. Stability against fission of heavy nuclei has been investigated by analyzing experimental data on both fission and evaporation residue (ER) cross-sections from heavy ion induced fusion-fission reactions and also from isotopic

distributions of the production cross-sections of various elements in high energy heavy ion fragmentation experiments.

Another interesting features of heavy ion induced fusion-fission reactions is the observation that for CN at high excitation energies (temperature >1 MeV), pre-scission multiplicity data of light particles and GDR γ point to a hindrance or slowing down of the fission process compared with that given by the transition-state theory of Bohr and Wheeler [5,6,10]. The fission hindrance is usually taken into account in statistical model calculations of CN decay by using the Kramers' expression for fission width which considers a dissipative dynamics for fission. However, it is often found that the pre-scission multiplicities (of evaporated particles and γ) and ER cross-sections can not be reproduced with the same strength of dissipation. A larger value of fission width is found necessary for ER cross-sections than those required to fit pre-scission multiplicities. This is reflected in smaller values of dissipation strength obtained from ER studies than those from analyses of pre-scission multiplicity data. For a number of systems, enhancement of fission width is achieved by reducing the height of the liquid drop model (LDM) fission barrier. The above observations suggest that improvements in fission modeling are necessary where effects such as the roles of excitation energy and shape (of the CN) dependence of dissipation need to be further investigated. Experimental data on both pre-scission multiplicities and ER cross-sections of a large number of systems are therefore required for a better understanding of the fission process

^a Corresponding author: bivash@pu.ac.in

of heavy nuclei with large excitation energies. With these above two broad motivations in mind, a series of experiments were performed to measure the ER excitation functions for $^{19}\text{F}+^{194,196,198}\text{Pt}$ (beam energies in the range of 101-137.3 MeV) and $^{16,18}\text{O}+^{194,198}\text{Pt}$ system (beam energies in the range of 77-106 MeV) at the HYRA spectrometer of IUAC, New Delhi Pelletron+LINAC accelerator facilities. The details of these experiments and results can be found in Ref. [5-13].

The paper is organized as follows. In Section 2 a general description of the experiment is given. In section 3 and 4 the results of $^{19}\text{F}+^{194,196,198}\text{Pt}$ and $^{16,18}\text{O}+^{194,198}\text{Pt}$ systems are described respectively. In section 5 the summary and conclusions are given.

2 Experimental Details

The experiments were performed at the 15 UD Pelletron accelerator facility of the Inter University Accelerator Centre (IUAC), New Delhi. Pulsed ^{19}F , ^{16}O and ^{18}O beams with a pulse separation of 4 μs (as ERs, produced at the target chamber, took about 3.5 to 4 μs to reach the focal plane, covering a distance of ~ 7.6 m.) was used in the experiment to bombard isotopically enriched ^{194}Pt and ^{198}Pt targets of thickness 260 $\mu\text{g}/\text{cm}^2$ and 170 $\mu\text{g}/\text{cm}^2$ each on 10 $\mu\text{g}/\text{cm}^2$ thick carbon backing, respectively. ER excitation function measurements were performed at laboratory beam energies of 101 to 137.3 for ^{19}F , 78.0 to 105.6 MeV for ^{16}O and 77.8 to 105.4 MeV for ^{18}O beam respectively. The heavy ERs produced in the reaction were separated from the intense beam background by the gas-filled HYRA spectrometer [4]. It is a dual-mode, dual-stage recoil mass separator and spectrometer. The present experiment was performed using the first stage of HYRA in the gas-filled mode. The electromagnetic configuration of the same is Q1Q2-MD1-Q3-MD2-Q4Q5 where Q stands for magnetic quadrupoles and MD stands for magnetic dipoles, respectively.

Elastically scattered Fluorine and Oxygen ions were detected in two silicon surface barrier detectors placed at $\pm 22.7^\circ$ with respect to the beam direction at a distance of 24.5 mm from target for monitoring and normalization of beam flux. The helium gas pressure in HYRA was set at 0.15 torr and HYRA magnetic field settings were calculated using a simulation program [13,14]. Low-energy ERs reaching the focal plane were detected using a position sensitive multiwire proportional counter (MWPC) having active area of 152.4×50.8 mm^2 . The MWPC was operated with isobutene gas of about 2 mbar pressure and it provides position signals (both X and Y positions), an energy signal from the cathode, and a timing signal from the anode. The position signals were taken from the two ends of the X and Y frames through delay-line chips. These were processed through constant fraction discriminators and were fed to the time-to-digital converter as stop signals, with the anode timing as the common start. The data were collected and analyzed using the IUAC data-sorting software CANDLE [16]. At each energy point, magnetic field values were also optimized by maximizing the ER yield at the focal plane, keeping the pressure fixed at 0.15 Torr. To get the time of

flight signal, the start signal was taken from the focal plane MWPC anode and stop signal was taken from RF used for beam pulsing. The logical OR signal of the two monitor detectors and the MWPC anode was taken as the master strobe for the data acquisition system. A TAC spectrum was finally recorded by taking the start from the MWPC-anode signal and stop from the RF signal. A two dimensional plot was generated between the TAC and the cathode of MWPC for separating the ERs reaching the focal plane from other background particles.

The details of the analysis procedure and methods for obtaining ER cross sections can be found in Ref. [7,9,11].

3 The case for $^{19}\text{F}+^{194,196,198}\text{Pt}$ reactions

The main motivation for this experiment is to search for shell stabilization effect, or the lack of it, for neutron shell closure at $N=126$. We shall compare the measured excitation functions of ER cross-section of ^{213}Fr ($N=126$) with those of ^{215}Fr ($N=128$) and ^{217}Fr ($N=130$) compound nuclei. We also perform statistical model calculations to analyze the data. The measured cross sections for the three systems are plotted in Figure 1. It is observed that the ER cross sections of ^{213}Fr are substantially smaller as compared with ^{215}Fr and ^{217}Fr .

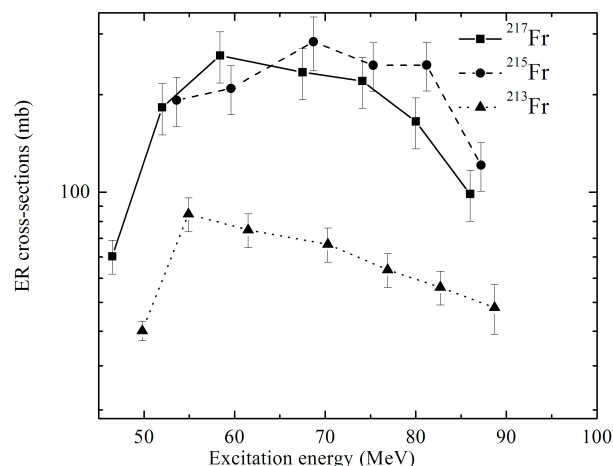


Figure 1. The excitation function of ER cross sections for different isotopes of Fr.

We next perform statistical model calculations for the interpretation of the ER data. The detail of the calculations can be found in Ref. [7]. We obtained the experimental survival probability as the ratio of the experimental ER cross-sections and the CCDEF predicted fusion cross-sections for all the Fr isotopes under study (see Figure 2 (a)). It is observed that the survival probability of all the isotopes decreases with increase in excitation energy, as expected. However, the survival probability is substantially smaller for the shell closed ^{213}Fr compared with the other two non-shell closed nuclei, ^{217}Fr and ^{215}Fr which are of comparable magnitudes. This finding is somewhat contrary to the expectation that a closed shell nucleus should be more stable against fission compared with the neighboring non-closed shell nuclei. The ratio of the survival probabilities of ^{217}Fr and ^{215}Fr with respect to ^{213}Fr are also obtained and are shown in Figure 2 (b). It is observed that the

survival probability of both ^{217}Fr and ^{215}Fr with respect to that of ^{213}Fr increases with increase of excitation energy.

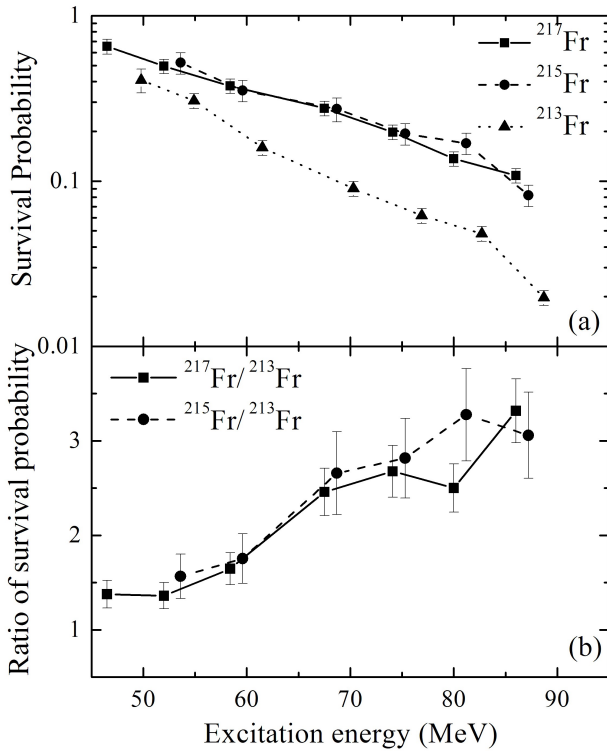


Figure 2. (a). The excitation function of survival probability for different isotopes of Fr. (b) Ratio of survival probabilities of ^{217}Fr and ^{215}Fr with respect to ^{213}Fr .

We next compared the above trends in the survival probability of the Fr nuclei with the predictions of statistical model calculations. The finite-range rotating liquid drop model (FRLDM) [21] potential is first used to calculate the fission barriers. The FRLDM barriers of $^{213,215,217}\text{Fr}$ nuclei for $l=0$ are obtained as 7.66, 7.90 and 8.12 MeV respectively. The ^{213}Fr nucleus is thus more unstable against fission compared with the other two Fr isotopes according to the FRLDM potential and the statistical model predictions of the ratio of the survival probability of ^{217}Fr and ^{215}Fr with respect to ^{213}Fr using the FRLDM fission barriers are shown in Figure 3 (a). When compared with the experimental trends given in Figure 2 (b), it is evident that the statistical model with FRLDM barriers grossly underestimates the ratios of the survival probabilities.

Following the prescriptions in Ref. [6]. We applied an excitation energy dependent shell correction to the FRLDM fission barriers. Statistical model calculations are then performed using the shell corrected fission barriers. The calculated ratios of the survival probabilities of ^{217}Fr and ^{215}Fr with respect to ^{213}Fr are shown in Figure 3 (b). It is observed that the statistical model calculations with shell corrected fission barriers also considerably under predict the ratios of experimental survival probabilities. From the above two plots it is observed that the FRLDM fission barriers obtained with or without shell correction cannot reproduce the relative survival probabilities of ^{217}Fr and ^{215}Fr nuclei with respect to ^{213}Fr . We therefore introduce a scaling factor K_f for the FRLDM barrier and treat it as an adjustable parameter to

fit the experimental ER cross-sections. It is found that a single value of K_f could not reproduce the Excitation functions of the different isotopes under study.

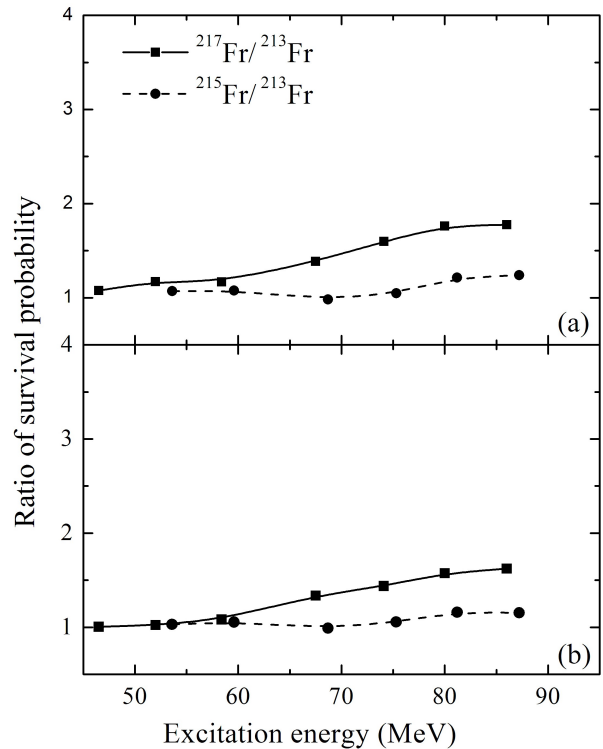


Figure 3. (a). The ratio of survival probability of ^{217}Fr and ^{215}Fr with respect to ^{213}Fr using FRLDM fission barriers. (b) Same as above but using shell corrected FRLDM fission barriers.

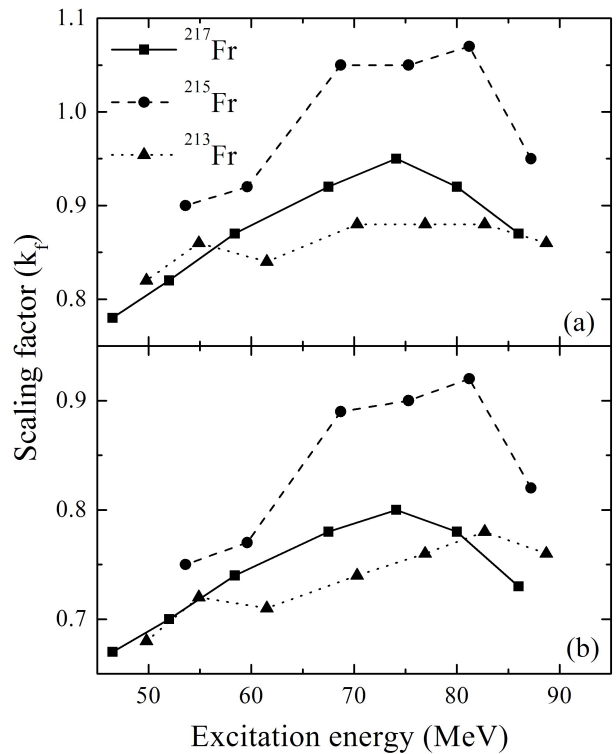


Figure 4. (a). The best fit K_f values obtained by fitting the experimental ER cross section with statistical model calculations using LDM fission barrier. (b) Same as above but using shell corrected fission barrier.

Finally, we fitted the experimental ER cross-sections by varying the value K_f at each excitation energy and

obtained the excitation energy dependent values of K_f for each CN. The excitation energy dependence of K_f for all the three CN obtained with and without shell correction in fission barrier is given in Figure 4 (a). In both the cases, we find an increasing trend in K_f values with increase in excitation energy for all the three isotopes of Fr. We also note an isotopic dependence of K_f values where the scaling factor for ^{213}Fr has the lowest value at most of the excitation energies whereas its values for ^{215}Fr are the largest of the three nuclei. The present results therefore indicate a steeper fall in barrier height with decrease in neutron number than that predicted by the FRLDM for Fr isotopes with neutron numbers ≥ 126 . A similar observation was made by Sagaidak et al. [16] for Po isotopes with neutron numbers ≤ 126 . It may however be remarked here that the same scaling factor is applied to the FRLDM barriers of all the daughter nuclei formed during the evaporation process and hence, the fitted values of K_f reflect the combined effect of barrier scaling in all the nuclei in a decay chain and do not represent the best-fit barrier for the original CN in particular.

4 The case for $^{16,18}\text{O}+^{194,198}\text{Pt}$ reactions

The main motivation of this set of experiments is to further explore the discrepancy between the dissipation strengths required to fit pre-scission multiplicities and ER cross-sections as mentioned in the introduction. We measured the excitation functions of ER cross-sections for the reactions $^{16,18}\text{O}+^{198}\text{Pt}$ in the present experiment. The pre-scission neutron multiplicities for the same systems have been reported in an earlier work [10]. We perform statistical model analysis of the measured ER cross-sections using the Kramers' fission width where we treat the dissipation strength as a free parameter to fit the ER excitation functions. The dissipation strengths obtained in the present work are compared with those obtained earlier from analysis of pre-scission neutron data [10].

The excitation functions of the measured ER cross sections for the $^{16,18}\text{O}+^{198}\text{Pt}$ reactions are given in Figure 5 (a). The ER excitation function for the previously measured [9] $^{16}\text{O}+^{194}\text{Pt}$ system is also shown in this figure for the sake of comparison. The data shows that ER cross section increases with increasing values of N/Z of the compound nuclei in an isotopic chain. Similar observation was made earlier for other systems [18,19]. The survival probabilities of the compound nuclei ^{214}Rn and ^{216}Rn formed in the $^{16,18}\text{O}+^{198}\text{Pt}$ reactions are next shown in Figure 5 (b). An increase in survival probability with neutron number in the CN is also observed here.

We next performed statistical model calculations following the formalism of Ref. [20]. The fission width is calculated following the work of Kramers [5,6] where the dynamics of the fission degrees of freedom is considered similar to that of a Brownian particle in a heat bath. The driving force in a thermodynamical system like a hot nucleus is provided by the free energy of the system. The free energy F is given by the Fermi gas model as

$$F(q, T) = V(q) - a(q)T^2 \quad (1)$$

Where (q) represents the collective coordinates and the collective potential $V(q)$ is obtained from the finite range liquid drop model [21]. The rotational energy of the compound nucleus is obtained using the shape-dependent rigid body moment of inertia and is included in the FRLDM potential. In the above equation, $a(q)$ is the level density parameter which depends on the shape of the compound nucleus specified by the collective coordinates (q) .

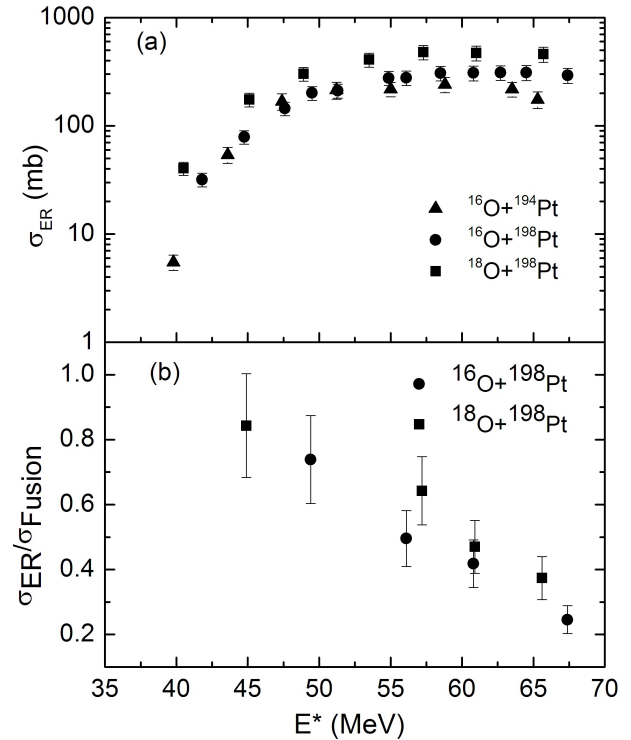


Figure 5. Variation of (a) ER Cross-section and (b) ER survival probability with excitation energy for $^{16,18}\text{O}+^{198}\text{Pt}$ systems.

Evaporation residue cross-sections are calculated in the statistical model for different values of the dissipation coefficient (β) for both the reactions under study and the results are given in Figure 6 and 7 along with the experimental values.

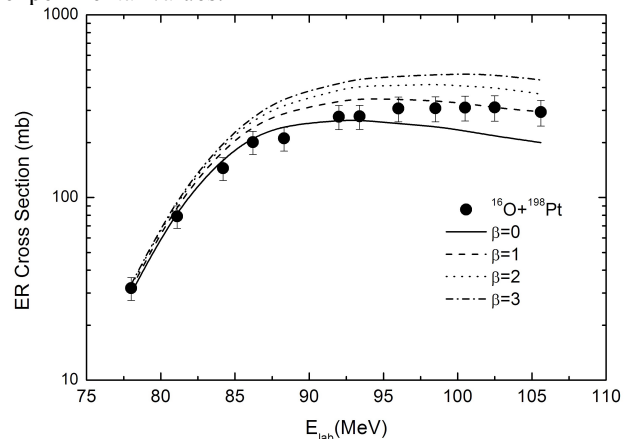


Figure 6. Calculated ER excitation functions for different values of β (in unit of 10^{21} s^{-1}) along with the experimental values for the $^{16}\text{O}+^{198}\text{Pt}$ reaction.

It is observed that good overall fits to the experimental excitation functions can be obtained with $\beta \sim (0-1) 10^{21} \text{s}^{-1}$ for the reaction $^{16}\text{O}+^{198}\text{Pt}$ forming the compound nucleus ^{214}Rn and $\beta \sim (1-2) 10^{21} \text{s}^{-1}$ for $^{18}\text{O}+^{198}\text{Pt}$ leading to the compound nucleus ^{216}Rn . On the other hand, dissipation strengths required to fit the pre-scission neutron multiplicities for the systems $^{16}\text{O}+^{198}\text{Pt}$ and $^{18}\text{O}+^{198}\text{Pt}$ lie in the range $(1-5) 10^{21} \text{s}^{-1}$ [10]. Clearly, smaller values of dissipation strength fit the ER cross-sections than those required for the pre-scission neutron multiplicities.

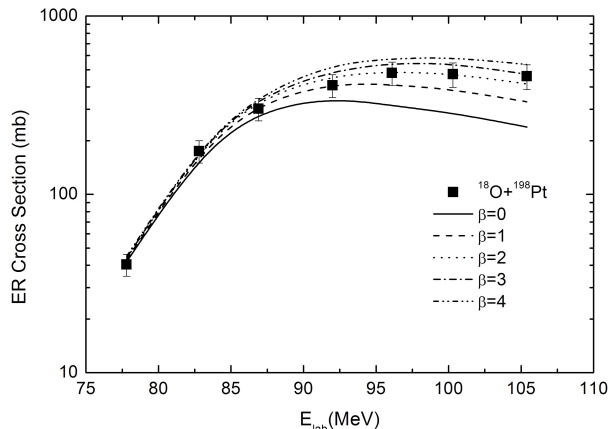


Figure 7. Calculated ER excitation functions for different values of β (in unit of 10^{21}s^{-1}) along with the experimental values for the $^{18}\text{O}+^{198}\text{Pt}$ reaction.

5 Summary and Conclusions

Recent results of ER excitation functions for $^{19}\text{F}+^{194,196,198}\text{Pt}$ and $^{16,18}\text{O}+^{194,198}\text{Pt}$ systems measured at HYRA spectrometer at IUAC are summarized. Detail statistical model calculations are performed for the interpretation of the data. Comparison of the survival probabilities of the compound nuclei derived from the experimental data shows that for ^{213}Fr with $N = 126$ has lower stability against fission compared with ^{215}Fr and ^{217}Fr with neutron number $N = 128$ and 130 respectively. From the statistical model analysis of the ER cross sections it is found that a scaling of the FRLDM fission barrier is necessary to fit the experimental data. The fitted scaling factors for ^{213}Fr are found to be smaller than compared with the other two nuclei in the entire excitation energy range. This feature is in clear disagreement with the theoretical predictions where fission barrier for closed-shell nuclei are found to be larger than those of the neighboring non-closed-shell nuclei. A further detailed study of the ingredients of the statistical model is necessary.

Statistical model analysis of the ER cross sections for $^{16,18}\text{O}+^{194,198}\text{Pt}$ systems shows that dissipation in fission dynamics is necessary to fit the experimental data. The fitted values of dissipation coefficient are however found to be smaller than those required to fit the pre-scission neutron multiplicities measured in a previous experiment [10] for the same systems. It is of further interest to note that while the pre-scission multiplicity increases marginally for $^{18}\text{O}+^{198}\text{Pt}$ compared with the $^{16}\text{O}+^{198}\text{Pt}$ system, the increase in ER cross section is substantial. This fact is reflected in the best-fit values of the

dissipation coefficient. While the isotopic dependence of dissipation strength for pre-scission neutrons is small [10], the dependence is large for ER cross sections as we find in the present work

Acknowledgments

This work was carried out at HYRA facility of IUAC, New Delhi. This talk comprises part of the Ph.D. thesis work of Dr. Varinderjit Singh and Dr. Rohit Sandal from Panjab University, Chandigarh. The author is thankful to Dr. N. Madhavan, Dr. S. Nath, Mr. J. Gehlot, Dr. Varinderjit Singh, Dr. Rohit Sandal, Mr. A. Jhingan, Mr. T. Varughese, Ms. K.S. Golda, Dr. P. Sugathan, Ms. Maninder Kaur, Ms. Gurpreet Kaur, Ms. Priya Sharma, Ms. Savi Goyal, Dr. S. Mandal, Dr. S. Verma, Dr. A. Saxena, Dr. S. Kailas, Dr. K. Mahata, Dr. S. Santra, Dr. A.M. Vinod Kumar, Dr. K.M. Varier, Dr. E. Prasad, Dr. A. Kumar, Dr. H. Singh, Dr. K.P. Singh, Dr. S. Muralithar, Dr. R.P. Singh, Dr. Santanu Pal, Dr. Jhilam Sadhukhan and Dr. A. Roy for helping in various aspects of this project.

References

1. P. Frobrich *et al.*, Nucl. Phys. A **563**, 326 (1993).
2. W. Ye, Phys. Rev. C **81**, 011603 (2010).
3. Y. Oganessian, J. Phys. (London) G **34**, R 165 (2007).
4. N. Madhavan *et al.*, PRAMANA J. Phys. **75**, 317 (2010); N. Madhavan *et al.*, Eur. Phys. J. Web of Conferences **17**, 14003 (2011).
5. Varinderjit Singh *et al.*, Phys. Rev. C **86**, 014609 (2012).
6. Varinderjit Singh *et al.*, Phys. Rev. C **87**, 064601 (2013).
7. Varinderjit Singh *et al.*, Phys. Rev. C **89**, 024609 (2014).
8. Varinderjit Singh *et al.*, Proc. DAE Symp. Nucl. Phys., Vol **57**, 428 (2012).
9. E. Prasad *et al.*, Phys. Rev. C **84**, 064606 (2011).
10. Rohit Sandal *et al.*, Phys. Rev. C **87**, 014604 (2013).
11. Rohit Sandal *et al.*, Phys. Rev. C (submitted)
12. Rohit Sandal *et al.*, Proc. DAE Symp. Nucl. Phys., Vol **57**, 532 (2012)
13. Rohit Sandal *et al.*, Proc. DAE Symp. Nucl. Phys., Vol **58**, 526 (2013)
14. S. Nath, A Monte Carlo code to model ion transport in dilute gas medium (unpublished).
15. S. Nath, Comput. Phys. Commun. **180**, 2392 (2009).
16. E.T. Subramaniam *et al.*, Collection and Analysis of Nuclear Data using Linux network (unpublished).
17. R.N. Sagaidak *et al.*, Phys. Rev. C **79**, 054613 (2009).
18. R.J. Charity *et al.*, Nucl. Phys. A **457**, 441 (1986).
19. R. Rafiei *et al.*, Phys. Rev. C **77**, 024606 (2008).
20. Gargi Chaudhuri *et al.*, Phys. Rev. C **65**, 054612 (2002).
21. A. J. Sierk, Phys. Rev. C **33**, 2039 (1986).